J. Earth Planet. Sci. Nagoya Univ., Vol. 54, 13 to 35, 2007

Lanthanide tetrad effect of Naegi granite-pegmatite suite, central Japan: Convex tetrad effect by fractional loss of fluid from hydrous felsic melt

Takafumi TAKAHASHI[1], Kazuya TANAKA[2] and Iwao KAWABE*

Department of Earth and Planetary Sciences, Graduate School of Environmental Studies, Building-E of Faculty of Science, Nagoya University, Chikusa, Nagoya 464-8602, Japan
(Received November 10, 2007 / Accepted December 27, 2007)

ABSTRACT

The Late Cretaceous (*ca.* 67 Ma) Naegi granite-pegmatite suite in Nakatsugawa City, Gifu Prefecture, central Japan, has been studied in view of the lanthanide tetrad effect in evolved felsic rocks. The pegmatite occurring sparsely in the granite body as small patches (<20 cm) and the matrix granite were sampled. REE including Y, major and some minor elements in the samples have been determined. The REE data for mineral separates (quartz, plagioclase, K-feldspar, biotite, and residual heavy minerals) from a granite sample have also been obtained. The chondrite-normalized REE patterns for pegmatite and granite commonly show convex tetrad effects and huge negative Eu anomalies of $Eu/Eu^* = 0.02-0.004$ but no notable Y/Ho fractionation. The whole-rock sample of granite and its mineral separates show similar convex tetrad effects, suggesting the convex tetrad effect in the original magma before crystallization. The granite and pegmatite show no significant differences in major element chemistry and mineralogy except mineral size and texture, but the pegmatite is depleted in Eu, Sr, and Ba relative to the granite. In addition, the pegmatite exhibits a convex tetrad effect and a fairly large negative Eu anomaly, when normalized by the granite. The field occurrence of pegmatite suggests a heterogeneous distribution of aqueous fluid inside of the granitic magma, which is possibly related to the unmixing phenomenon of fluid and silicate melt. Here is proposed a simple model of fractional loss of fluid from hydrous felsic melt. Applying the model to the observed REE fractionation between pegmatite and host granite pairs, REE partition coefficients between aqueous fluid and melt, K_d(REE: fluid/melt), have been evaluated. The $\log K_d$(REE: fluid/melt) values indeed exhibit small concave tetrad effects, positive Eu anomalies, and light REE enrichment trends. Fractional loss of fluid from a hydrous felsic melt system leaves residual silicates in which the small concave tetrad effect and positive Eu anomaly of logKd(REE: fluid/melt) can be exaggerated in reversed manners. As a result, the residual silicates acquire pronounced convex tetrad effects and huge negative Eu anomalies.

[1] Present address: Research Laboratory for Nuclear Reactors, Tokyo Institute of Technology, 2-12-10 O-okayama, Meguro-ku, Tokyo 152-8550, Japan
[2] Present address: Department of Earth and Planetary Systems, Graduate School of Science, Hiroshima University, Kagamiyama, 1-3-1, Higashi-Hiroshima 739-6526, Japan
*The corresponding author. E-mail: kawabe@eps.nagoya-u.ac.jp

INTRODUCTION

The lanthanide tetrad effects are observed in the chondrite-normalized REE patterns for felsic igneous rocks like granites and rhyolites as well as highly evolved felsic rocks including pegmatites and leuco-granites (Masuda and Akagi, 1989; Zhao *et al.*, 1992; Lee *et al.*, 1994; Kawabe, 1995; Bau, 1996; Irber, 1999). Interestingly such tetrad effects are commonly convex ones, i.e. the M-type tetrad effects in the classification by Masuda *et al.* (1987). In addition, large negative Eu anomalies are always associated with the tetrad effects. This situation has been further confirmed in the recent studies of Chinese Woduhe, Baerzhe and Qianlishan granites (Jahn *et al.*, 2001; Zhao *et al.*, 2002), German Li-F granite (Monecke *et al.*, 2002), Japanese Toki granite (Takahashi *et al.*, 2002) and our preliminary result for Japanese Naegi granite-pegmatite suite (Takahashi and Kawabe, 2003).

The tetrad effect was first proposed by Peppard *et al.* (1969) on the basis of experimental logarithmic distribution coefficients for REE(III), $\log K_d$(REE), in the liquid-liquid extraction systems. Jørgensen (1970) and Nugent (1970) independently pointed out that the tetrad effects are explained by Jørgensen's (1962) equation for the inter-electron repulsion energies for the ground-terms of $[4f]^q$ configurations and by the spectroscopically known nephelauxetic effect. Jørgensen's (1962) equation is presently called the refined spin-pairing energy theory (RSPET) as in Jørgensen (1979). Spectroscopic analyses of f→f transition energies of REE(III) compounds and complexes indicate that the inter-electronic repulsion energies for the ground-terms of $[4f]^q$ configurations, which are expressed by Racah (E^1 and E^3) parameters, are slightly but systematically smaller than those of gaseous free REE^{3+} ion series. For example, the Racah parameters for Nd^{3+} decrease from NdF_3 to $NdCl_3$, $NdAlO_3$, and then to $NdO_{1.5}$ (Caro *et al.*, 1981). This series is called the nephelauxetic series, and it implies the increasing covalency of REE^{3+} ion in condensed phases in this order because of interactions of REE^{3+} with different ligands (Reisfeld amd Jørgensen, 1977). The differences of Racah parameters for REE^{3+} ion between a pair of REE(III) compounds or complexes become visible as a zig-zag variation of $\log K_d$(REE) for the solvent extraction systems (Jørgensen, 1979).

Kawabe (1992) improved the RSPET equation and applied it to the series variations of lattice energies of $REEO_{1.5}$ and $REEF_3$ and ΔH_r for the ligand-exchange reaction of REE^{3+} between the oxide and fluoride series. He successfully explained the reason why the ionic radii for REE^{3+} with the coordination number (CN)=6 show a tetrad effect but those radii for REE^{3+} with CN=8 do not from the different Racah parameters (E^1 and E^3) among $REEO_{1.5}$, $REEF_3$ and gaseous free REE^{3+} ion series. It has also been shown that relative differences of Racah parameters (E^1 and E^3) between $REEO_{1.5}$ and $REEF_3$ series estimated from their thermo-chemical data by using the improved RSPET equation are consistent with the spectroscopically known Racah parameters (E^1 and E^3) for $NdO_{1.5}$ and NdF_3. The improved RSPET equation was successfully applied to the experimental data by Peppard *et al.* (1969) as well as to $\log K_d$(REE) data for low temperature geochemical REE partitioning systems (Kawabe and Masuda, 2001 and references therein).

Although our understanding of lanthanide tetrad effects in low-temperature

geochemical systems has advanced significantly, the tetrad effects in geochemical materials produced in high temperatures are not well understood yet, in particular, the convex tetrad effects observed frequently in felsic igneous rocks. There is no consensus about what a mechanism can produce the marked convex tetrad effect in evolved felsic rocks. Majority of researchers, however, referred to the importance of "water/rock" and "fluid/melt" interactions, because relatively large differences in Racah parameters (E^1 and E^3) for REE^{3+} are expected for the pair of aqueous fluid and silicate melt or minerals than the pairs of silicate melt and silicate minerals (Kawabe, 1995; Irber, 1999; Jahn *et al.*, 2001). Recently Zhao *et al.* (2002) reported an important observation that convex tetrad effects and strong Eu depletion are present in both whole-rock samples and their constituent minerals of Quanlishan and Baerzhe granites in China. They argued that felsic hydrous magama had the convex tetrad effect before crystallization, and that the fluid/melt interaction is the most important agent to produce the convex tetrad effect. In order to gain further insight into this problem, we have studied the Naegi granite-pegmatite suite and the preliminary results have been reported (Takahashi and Kawabe, 2003). The aim of this paper is to present more detailed results and discussion as to the origin of lanthanide tetrad effects of the Naegi granite-pegmatite suite.

SAMPLES AND EXPERIMENTAL

The Naegi granite-pegmatite suite distributes over the eastern part of Mino district in the inner zone of central Japan (Fig. 1). The Naegi granite and pegmatite were sampled at a quarry pit in Yawata districkt, Naegi, Nakatugawa city, Gifu prefecture. In this area, Nohi rhyolite, Naegi granite, Paleozoic clastics and granite porphyry distribute. The Naegi granite crops out in a basn-like lowland surrounded by Nohi rhyolite and granite porphyry. According to Shibata *et al.* (1962), the K-Ar age of Naegi granite is 64-68 Ma. Suzuki *et al.* (1994) reported the CHIME age of monazites of Naegi granite of 67 Ma.

The Naegi granitic rocks in Yawata district are fine to medium-grained biotite granites. Pocket-like pegmatite patches, mostly not greater than 20 cm in size, occur sparsely in the granite body of the quarry pit. Pegmatites are rather compact and have no significant central cavities. In some of pegmatites there exist fine-grained materials (FMA) in the border zones between coarse-grained pegmatite and host granite. We will distinguish FMA from pegmatite and granite in the study. All the specimens sampled at the quarry pit were cut by diamond saw in order to separate pegmatite parts from granite hosts. Two specimens (NG10 and NG11) were cut into three parts of granite, FMA and pegmatite. The granite samples are mainly composed of smoky quartz, K-fedspar, plagioclase and small amounts of biotite. The average mode of constituent minerals is 46% of quartz, 34.7% of K-feldspar, 15.1% of plagioclase and 3.9% of biotite. Although pegmatite samples exhibit coarse-grained textures, their essential mineral assemblages are almost the same as those of granite samples. Both granite and pegmatite samples contain topaz, zircon, monazite, fluorite and mica as accessory minerals. Under petrographic microscope, it is observed that biotite often has pleochroic halos.

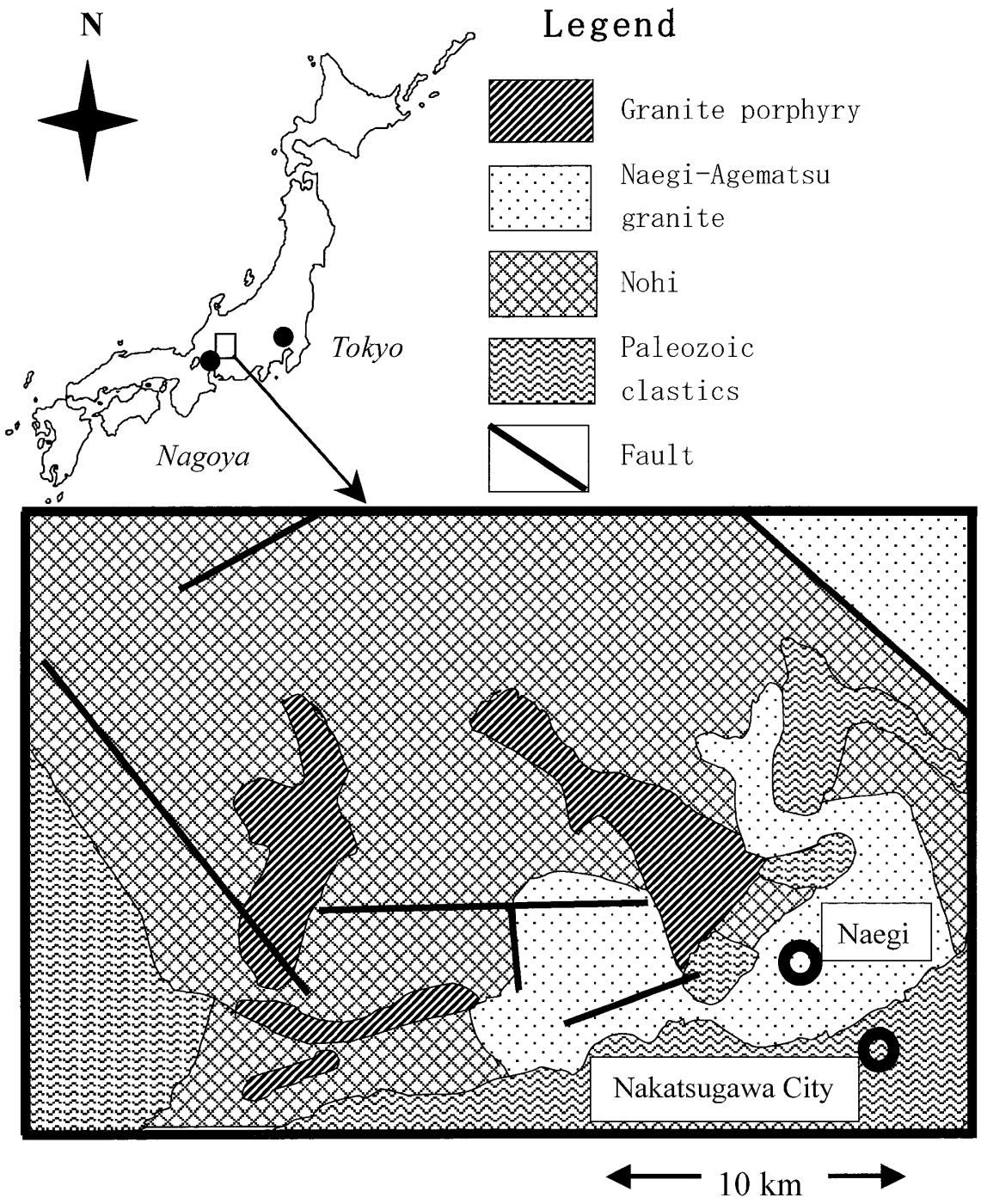

Fig. 1 Simplified geologic map of Naegi Area, Nakatugawa city, Gifu Prefecture, central Japan.

The constituent minerals (quartz, plagioclase, K-feldspar, biotite, and residual heavy minerals) of a granite sample (NG9-1) were separated by heavy liquids of bromoform and methylene iodide. When necessary, both heavy liquids were diluted by acetone. Their density values were always checked by a set of glass beads with known densities. As the first step, pulverized samples with 180~250 μm in size were separated

into felsic and mafic minerals by using bromoform of 2.8 g/cm^3. The felsic minerals further separated into the three fractions of quartz, K-feldspar and plagioclase by using diluted bromoform solutions. The mineral fraction with densities greater than 2.8 g/cm^3 were further separated into biotite and the other heavier fraction designated collectively as heavy minerals here by methylene iodide. Mineral separates were checked by XRD. An aliquot of the heavy mineral fraction was cemented in epoxy-resin on a slide glass and polished for EPMA-EDS observation. The individual mineral grains were identified by EPMA-EDS. Although biotite is still abundant in the heavy mineral fraction, the following accessory minerals were identified; yttrofluorite, zircon, topaz, and muscovite. Each mineral separate was further pulverized by using a pestle when it is used for chemical analysis.

The determinations of REE including Y for whole-rock and mineral separate samples were made according to the ICP-AES method combined with pre-concentration technique (Kawabe, 1995). For the determinations of less abundant REE (Pr, Tb, Ho and Tm), an ultrasonic nebulizer was used (Kawabe *et al.*, 1995). ICP-AES determinations of Sr and Ba were made by using separate sample solutions prepared by HF-mineral acid ($HClO_4$ and HNO_3) digestion of powder samples. Major element analyses were carried out by XRF method, in which glass beads prepared by fusing the mixture of pulverized samples (0.7 g) and lithium tetraborate (6.0 g) were used.

RESULTS AND DISCUSSION

1) Analytical results

The analytical results of major elements, Sr amd Ba are listed in Table 1. The REE and Y analyses for whole-rock samples of granite, pegmatite and FMA are summarized in Table 2. The REE and Y analyses of mineral separates (quartz, plagioclase, K-feldspar, biotite, and residual heavy minerals) from a granite sample (NG9-1) are listed in Table 3.

2) Chondrite-normalized REE patterns for whole-rock samples

The chondrite-normalized REE patterns for whole-rock samples of granite, pegmatite and FMA are shown in Figs. 2, 3 and 4, respectively. The chondritic REE data are those for CI chondrite by Anders and Grevesse (1989), but Tb, Ho and Tm values are by Ebihara (2002, personal communication). These chondritic REE data are listed in the last column of Table 3. Discussion about Tb, Ho and Ho abundances in CI chondrite has been given elsewhere (Tanimizu and Tanaka, 2002; Yamamoto *et al.*, 2005). The REE patterns for all the granite samples are quite alike with each other, so that we have classified them into three groups according to their REE concentrations, and then calculated averaged REE abundances for the three groups by using their geometric means. The average No. 1 is for three samples with higher REE concentrations (NG6-1, 6-2, and 14-3), the average No.2 is for eight samples with intermediate REE concentrations (NG2-1, 4-5, 5-2, 10-1, 11-1, 14-1, 14-2, and 14-5), and the average No. 3 is for five samples with lower REE concentrations (NG1-2, 1-3, 9-1, 14-4 and 16-2). The chondrite-normalized REE abundance patterns for the three averaged data of granite samples are shown in Fig. 2.

Table 1 Analytical results of major elements, Sr and Ba.

Sample	SiO2(%)	Al2O3(%)	Fe2O3(%)	TiO2(%)	MnO(%)	MgO(%)	CaO(%)	Na2O(%)	K2O(%)	P2O5(%)	H2O(-)(%)	H2O(+)(%)	Total(%)	Sr(ppm)	Ba(ppm)
NG1-2	74.14	12.81	1.05	0.037	0.023	0.06	0.64	5.30	5.08	0.009	0.17	0.07	99.4	15.1	25.2
NG1-3	73.97	12.90	0.983	0.03	0.02	0.057	0.57	5.17	5.46	0.01	0.10	0.25	99.5	9.81	20.4
NG2-1	75.49	12.52	1.204	0.048	0.056	0.031	0.64	5.09	4.75	0.012	0.02	0.04	99.9	10.8	21.6
NG4-5	75.09	12.89	1.114	0.038	0.028	0.07	0.72	4.29	4.87	0.01	0.10	0.20	99.4	10.5	22.0
NG5-2	73.42	13.21	1.13	0.049	0.025	0.065	0.86	4.18	4.28	0.01	0.15	0.23	97.6	9.59	28.6
NG6-1	74.23	13.05	0.972	0.038	0.025	0.06	0.81	4.20	4.49	0.01	0.08	0.28	98.2	10.6	24.9
NG6-2	74.30	13.15	1.098	0.047	0.026	0.061	0.78	3.99	4.65	0.009	0.20	0.18	98.5	20.5	454
NG9-1	74.42	12.24	1.055	0.039	0.025	0.052	0.69	5.08	4.39	0.009	0.05	0.16	98.2	4.55	25.4
PG9-2	74.45	12.79	0.8	0.018	0.024	0.044	0.52	5.40	4.58	0.007	0.03	0.14	98.8	1.52	9.14
NG10-1	72.95	13.09	0.989	0.041	0.023	0.061	0.81	4.12	4.50	0.006	0.06	0.18	96.8	9.84	60.3
FMA10-2	72.25	12.11	1.187	0.039	0.026	0.051	0.79	4.75	4.01	0.008	0.05	0.14	95.4	3.96	8.35
PG10-3	74.92	11.93	0.989	0.009	0.03	0.027	0.56	5.07	3.10	0.006	0.02	0.05	96.7	1.16	4.32
NG14-1	76.05	12.40	1.017	0.035	0.027	0.06	0.68	4.05	4.62	0.011	0.13	0.11	99.2	8.35	25.2
NG14-2	74.76	12.87	1.084	0.04	0.027	0.059	0.73	4.03	4.66	0.01	0.10	0.16	98.5	9.30	23.1
NG14-3	75.00	12.66	0.953	0.037	0.025	0.059	0.65	3.46	5.11	0.008	0.31	0.26	98.5	22.5	261
NG14-4	76.65	11.80	0.966	0.038	0.031	0.06	0.62	4.28	4.58	0.01	0.02	0.19	99.2	12.2	223
NG14-5	75.69	12.48	1.019	0.039	0.025	0.055	0.70	3.89	4.42	0.008	0.06	0.21	98.6	8.09	19.4
PG15-1	73.12	13.43	1.265	0.001	0.021	0.028	0.38	4.83	4.68	0.006	0.11	0.14	98.0	1.68	3.66
PG16-1	79.35	10.64	0.768	0.006	0.033	0.032	0.34	7.14	3.20	0.009	0.06	0.15	101.7	1.50	3.82
NG16-2	74.76	12.25	0.841	0.023	0.018	0.05	0.52	8.20	4.96	0.009	0.05	0.24	101.9	7.70	176

Table 2 REE and Y analyses (in ppm) for whole-rock samples of granite (NG), pegmatite (PG) and fine-grained material (FMA)*.

Sample	La	Ce	Pr	Nd	Sm	Eu	Gd	Tb	Dy	Ho	Er	Tm	Yb	Lu	Y	$TE_{1,3}$	Eu/Eu*
NG1-2	17.0	39.9	4.83	21.9	7.31	0.054	8.82	1.74	11.9	2.60	8.20	1.26	8.67	1.29	78.5	1.04	0.020
NG1-3	16.2	38.7	5.01	22.1	7.62	0.052	9.61	2.04	13.3	2.91	9.10	1.42	9.63	1.45	86.4	1.07	0.019
NG2-1	21.6	52.4	6.70	28.4	9.44	0.062	12.2	2.55	17.5	3.83	11.7	1.71	11.1	1.53	105	1.08	0.018
NG5-2	23.8	57.8	7.43	32.0	10.46	0.063	12.8	2.55	16.6	3.52	10.6	1.56	10.4	1.50	97.2	1.07	0.017
NG4-5	21.2	50.8	6.73	28.5	9.75	0.063	12.5	2.53	16.9	3.64	11.2	1.69	11.0	1.61	106	1.07	0.018
NG6-1	25.5	61.8	7.97	34.3	11.28	0.077	14.0	2.75	19.0	4.04	12.5	1.88	12.4	1.81	117	1.06	0.019
NG6-2	26.3	63.2	8.26	35.3	11.73	0.073	14.5	2.92	19.8	4.16	13.2	1.99	13.0	1.97	126	1.07	0.017
NG9-1	17.8	44.3	5.48	24.5	8.24	0.062	10.1	1.97	13.3	2.74	8.49	1.25	8.32	1.22	80.1	1.06	0.021
PG9-2	17.5	43.4	5.73	22.5	8.15	0.034	10.0	2.08	14.7	3.16	10.4	1.70	12.3	1.86	99.1	1.11	0.011
NG10-1	19.6	48.3	6.10	28.7	9.91	0.072	12.3	2.35	15.6	3.32	10.2	1.50	9.80	1.42	91.0	1.04	0.020
FMA10-2	8.33	19.9	2.97	14.9	6.28	0.037	9.13	1.76	12.7	2.79	8.59	1.24	8.05	1.17	81.9	1.01	0.015
PG10-3	16.9	40.1	5.20	21.5	9.25	0.026	13.2	3.12	24.0	5.68	19.9	3.35	23.8	3.59	217	1.09	0.007
NG11-1	23.6	64.1	7.88	32.0	10.68	0.070	12.8	2.54	16.4	3.51	10.7	1.59	10.4	1.53	91.1	1.11	0.018
FMA11-2	15.7	39.8	5.91	24.8	8.70	0.055	10.6	2.18	13.4	2.86	8.55	1.29	8.08	1.18	72.3	1.10	0.029
PG11-3	14.2	38.7	5.67	24.3	9.63	0.026	13.3	3.02	20.3	4.44	14.3	2.34	15.5	2.33	135	1.05	0.007
NG14-1	22.2	50.9	6.52	29.0	9.67	0.076	12.3	2.38	16.1	3.45	10.6	1.57	10.1	1.48	98.7	1.03	0.021
NG14-2	22.2	54.3	7.06	30.5	9.96	0.081	12.9	2.56	16.7	3.51	10.9	1.64	10.8	1.57	103	1.07	0.022
NG14-3	24.3	59.6	7.78	33.3	11.42	0.070	14.5	2.85	19.1	4.07	12.6	1.94	12.8	1.89	121	1.07	0.017
NG14-4	16.1	38.0	4.55	20.5	6.73	0.071	8.48	1.60	11.0	2.33	7.26	1.08	7.07	1.05	66.6	1.03	0.029
NG14-5	22.9	55.8	7.10	30.3	10.19	0.072	12.3	2.49	17.2	3.58	11.1	1.68	11.0	1.63	106	1.08	0.020
PG15-1	11.6	27.5	3.41	13.2	5.08	0.013	6.38	1.46	10.7	2.47	8.14	1.39	10.3	1.55	73.2	1.10	0.007
PG16-1	21.2	56.5	7.52	28.2	10.93	0.016	13.7	3.48	26.0	5.96	21.6	4.11	32.5	5.23	181	1.18	0.004
NG16-2	12.5	31.4	4.13	18.9	7.28	0.039	9.67	1.92	13.8	2.95	9.27	1.39	9.25	1.36	83.9	1.06	0.014

) The last two columns are for the practical parameter (TE1, 3) for tetrad effect by Irber (1999) and the parameter for Eu anomaly, respectively. The Eu anomaly itself is given as log(Eu/Eu).

Table 3 REE and Y concentrations (ppm) in mineral separates from a Naegi granite sample (NG9-1) and the chondritic REE data for normalization accepted in this study.

	quar tz	K-feldspar	plagioclase	biotite	heavy minerals	CI chondrite*
La	1.53	7.13	4.45	106	121	0.2347
Ce	3.50	12.2	7.21	264	325	0.6032
Pr	0.458	1.19	0.686	33.1	42.7	0.0891
Nd	1.76	3.83	2.44	133	167	0.4524
Sm	0.657	1.13	0.845	37.7	60.0	0.1471
Eu	0.0043	0.100	0.027	0.048	0.029	0.056
Gd	0.833	1.24	1.22	43.3	74.7	0.1966
Tb	0.185	0.244	0.278	9.36	17.2	0.0348§
Dy	1.15	1.53	1.93	63.3	125	0.2427
Ho	0.260	0.305	0.398	13.9	28.8	0.0525§
Er	0.821	0.919	1.31	42.3	98.5	0.1589
Tm	0.132	0.137	0.184	6.40	18.4	0.0234§
Yb	0.877	0.903	1.25	39.6	153	0.1625
Lu	0.136	0.121	0.177	5.43	22.0	0.0243
Y	6.81	9.07	12.4	327	923	1.56

*) Data except for Tb, Ho , and Tm are in Anders and Grevesse (1989).
§) Data for Tb, Ho , and Tm are by Ebihara (2002, personal communication). Discussion on the acceptance of the three data can be found in Tanimizu and Tanaka (2002) and Yamamoto *et al.* (2005).

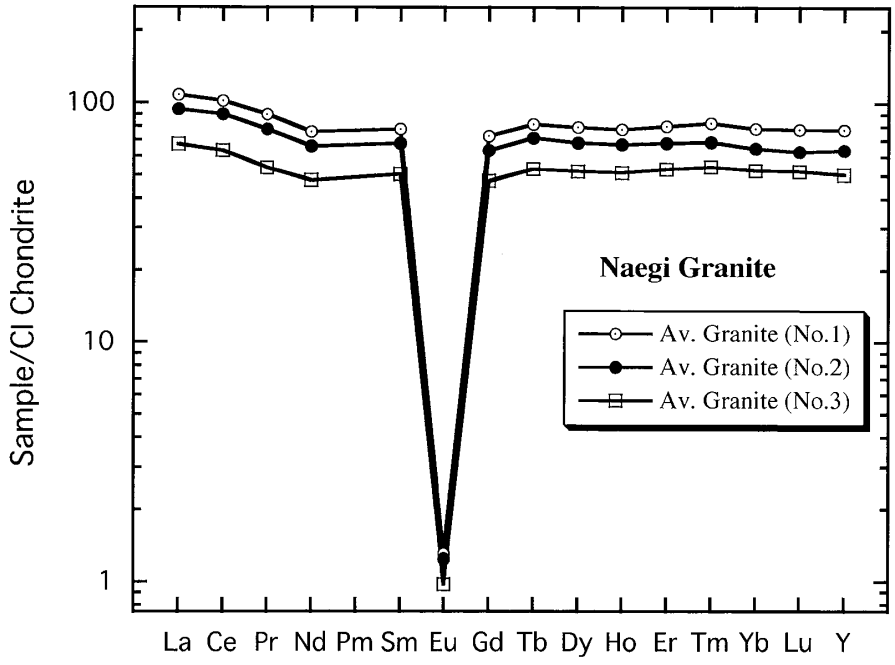

Fig. 2 The chondrite-normalied REE patterns for averaged Naegi granite samples calculated as the geometric means. The average No.1 is for three samples with higher REE concentrations (NG6-1, 6-2, and 14-3), the average No.2 is for eight samples with intermediate REE concentrations (NG2-1, 4-5, 5-2, 10-1, 11-1, 14-1, 14-2, and 14-5), and the average No. 3 is for five samples with lower REE concentrations (NG1-2, 1-3, 9-1, 14-4 and 16-2). Concave (M-type) tetrad effects and huge negative Eu anomalies are seen. The convexity in heavy REE is less marked when compared with that in light REE.

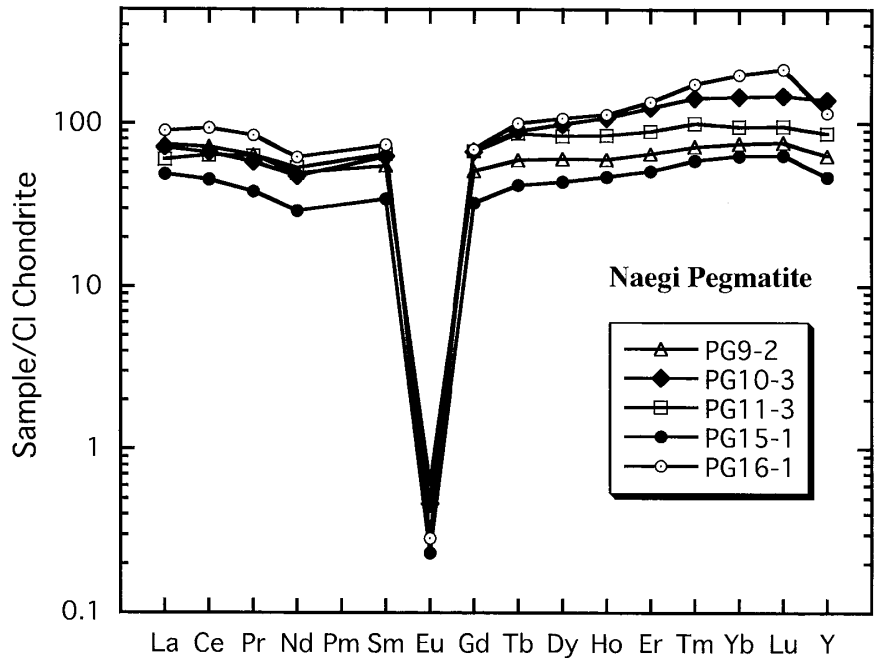

Fig. 3 The chondrite-normalized REE patterns for Naegi pecmatite samples. Convex (M-type) tetrad effects of pegmatites are more obvious than those of granite samples (Fig. 2). The heavy REE enrichment trend is also seen unlike the granite samples (Fig. 2).

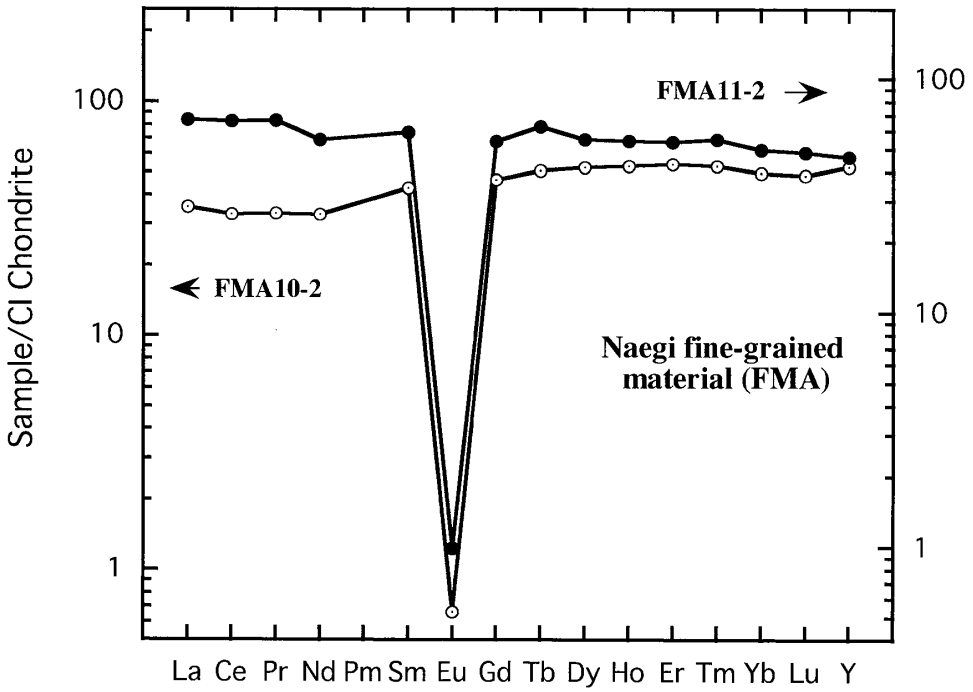

Fig. 4 The chondrite-normalized REE patterns for the fine-grained materials of Naegi granite-pegmatite suite. The REE pattern for FMA10-2 (open circles) suggests a small concave (W-type) tetrad effect feature.

The REE patterns of whole-rock granites show similar convex tetrad effects, which are the M type tetrad effects in the classification by Masuda *et al.* (1987). The convex-upward tetrad curves are evident for the first tetrad (La, Ce, Pr and Nd) and the third one (Gd, Tb, Dy and Ho). The second tetrad curves for Pm, Sm, Eu and Gd cannot be drawn immediately because of absence of Pm and the extremely large negative Eu anomalies ($Eu/Eu^* = 0.014-0.029$, see Table 2), but assuming that the second tetrad curve intersects with the first one at the mid point between Nd and Pm, we can draw the the second tetrad curve for Sm and Gd points. The fourth tetrad curves for Er, Tm, Yb and Lu, however, do not show notable curvatures. Therefore, the convex tetrad effects in the chondrite-normalized REE patterns for whole-rock granite samples are not quite regular.

The chondrite-normalized REE patterns for four whole-rock samples of pegmatites (Fig. 3) show similar features to those for the whole-rock granites (Fig. 2), but there can be recognized their differences: 1) the fourth tetrads indicate convex-upward curvatures more obviously in pegmatites than in granites, 2) there are heavy REE enrichment trends in pegmatites, whereas such trends are not in granites, and 3) the negative Eu anomalies of pegmatites ($Eu/Eu^* = 0.004-0.011$, see Table 2) are much larger than those of granites. These differences represent REE fractionation between pegmatite and granite.

The REE pattern for the finer-grained materials (FMA) in the border zones between coarse-grained pegmatite and host granite (NG10 and NG11) are different from those for granite and pegmatite (Fig. 4). The sample of FMA10-2 in the border zone between the granite (NG10-1) and pegmatite (PG10-3) appears to indicate concave-upward curves in the first and fourth tetrads. This is a diagnostic of W type tetrad effects by Masuda *et al.* (1987). This feature is not clear in the other sample of FMA11-2. We will discuss the REE characteristics of the finer-grained materials (FMA) in relation to the argument as to the origin of such a texture by Jahns and Burnham (1969) in the later subsection.

3) Depletion of Sr, Ba and Eu in pegmatite and no significant Y/Ho fractionation

There are no significant differences in major element composition between granite and pegmatite samples (Table 1), but Sr and Ba contents of pegmatite samples are significantly smaller than those of granite samples. These are correlating with the systematically larger negative Eu anomalies of pegmatite samples relative to granite ones (Fig. 5). Even though granite samples show huge negative Eu anomalies, pegmatite samples are much more depleted in Eu than granite ones. Pegmatite samples are also depleted in Sr and Ba than granite ones, suggesting that Eu(II), Sr and Ba which were more stable in aqueous fluid than in residual silicates were lost from the magmatic system. This is compatible with the large positive Eu anomalies observed in hydrothermal fluid issuing from the mid-oceanic ridges (Michard, 1989) and the distinct thermodynamic properties of Eu(II) and Eu(III) in high temperature aqueous solutions (Sverjensky, 1984).

Non-chondritic Y/Ho ratios in evolved felsic rocks are sometimes regarded as an indicator of magma/fluid interaction. Bau (1996) argued that, if geochemical systems are characterized by the CHARAC (Charge and Radius Control) trace element behavior,

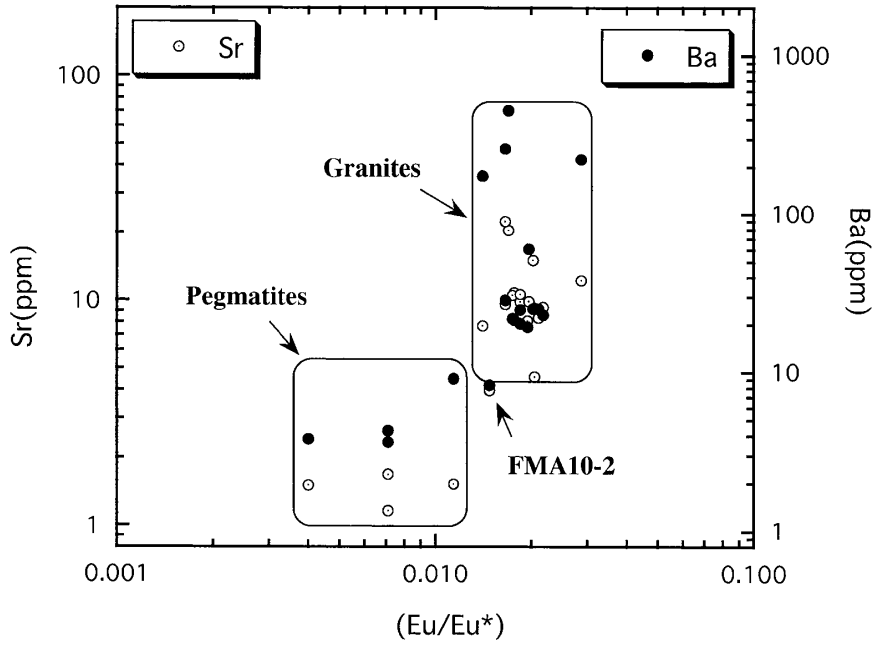

Fig. 5 Plot of Sr and Ba contents against Eu anomaly (Eu/Eu*) for Naegi granite, pegmatite and FMA samples. Pegmatite parts are more depleted in Eu, Sr and Ba than granite parts.

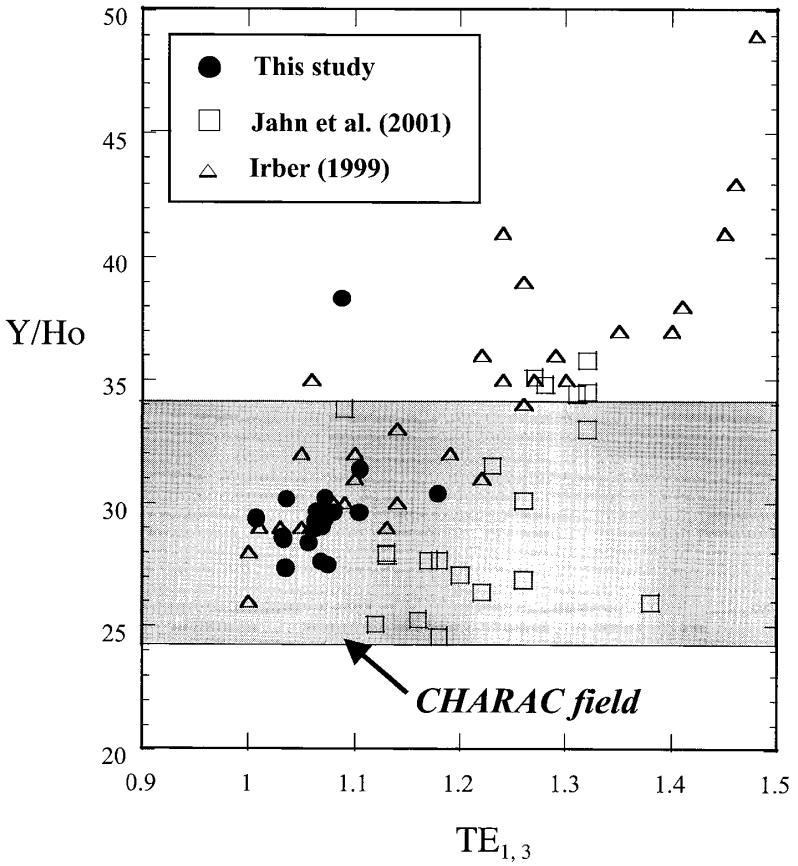

Fig. 6 TheY/Ho ratio plotted against the parameter of $TE_{1,3}$ (Irber, 1999) for Naegi granite and pegamtite samples. The German peraluminous granites (Irber,1999) and the Woduhe and Baerzhe granites (Jahn *et al*, 2001) are also plotted for comparison.

elements with similar charge and radius like Y-Ho and Zr-Hf pairs should display extremely coherent behavior and show the respective chondritic ratios. Indeed Y/Ho and Zr/Hf ratios of most of basic to intermediate igneous rocks are clustering around the chondritic Y/Ho and Zr/Hf ratios, and the CHARAC fields can be specified empirically. However, evolved igneous rocks sometimes indicate non-chondritic Y/Ho and Zr/Hf ratios. According to Bau (1996), the CHARAC behavior holds in pure silicate melt systems whereas the Non-CHARAC one does in highly evolved magmas enriched in water, Li, B, F, P and/or Cl. He put forwards that evolved felsic rocks like pegmatites and leucogranites with non-chondritic Y/Ho ratios show marked tetrad effects in their chondrite-normalized REE patterns. The Naegi granite and pegmatite display the convex (M type) tetrad effects, but most of their Y/Ho ratios are within the range of 27–30. In Fig. 6, the Y/Ho ratios of the Naegi granite and pegmatite samples are plotted against the practical parameter for tetrad effect of $TE_{1,3}$ by Irber (1999), together with the data for German peraluminous granites (Irber, 1999) and Chinese Woduhe and Baerzhe granites (Jahn *et al.*, 2001). The Naegi granite and pegmatite samples resembles Chinese Woduhe and Baerzhe granites in the diagram, in which very few samples are plotted in the Non-CHARAC field. There is no significant correspondence between non-chondritic Y/Ho ratios and tetrad effects, and Bau's (1996) argument does not hold in the cases of Naegi pegmatite and Woduhe and Baerzhe granites.

4) *Chondrite-normalized REE patterns for mineral separates of granite*

The chondrite-normalized REE patterns for mineral separates of quartz, plagioclase, K-feldspar, biotite, and residual heavy minerals from a granite sample (NG9-1) are shown in Fig. 7. The heavy minerals are the collection of biotite, yttrofluorite, zircon, topaz, and muscovite as described above. Each mineral separate show more or less similar convex tetrad effects and large negative Eu anomalies. In Fig. 8, respective mineral separates are normalized by the bulk granite of NG9-1, in which quartz, K-feldspar and plagioclase do not show significant tetrad effect variations whereas biotite and heavy mineral fractions still display small octad and tetrad effect variations, respectively. The contrasting REE patterns for mineral separates when normalized by chondrite and the bulk granite mean that the convex tetrad effect was present in the Naegi granite magma before crystallization. The present results are comparable with the REE data for whole-rock and mineral separate of Quanlishan and Baerzhe granites by Zhao *et al.* (2002), and support their argument that the fluid/melt interaction is the most important agent to produce the convex tetrad effect.

In Fig. 8, it is interesting that both K-feldspar and plagioclase display obvious positive Eu anomalies in contrast to the negative Eu anomalies of biotite and heavy minerals and no Eu anomaly of quartz. The REE enrichment patterns with sharp positive Eu anomalies of feldspars relative to the whole-rock granite are quite analogous to well-known REE partition coefficients between feldspars and melts (Drake and Weill, 1975: Henderson, 1984; McKay, 1989). Therefore significant fractions of Eu in feldspars were incorporated as Eu(II), and the dominant Eu in the aqueous fluid phase lost away from the Naegi magmatic system was also Eu(II).

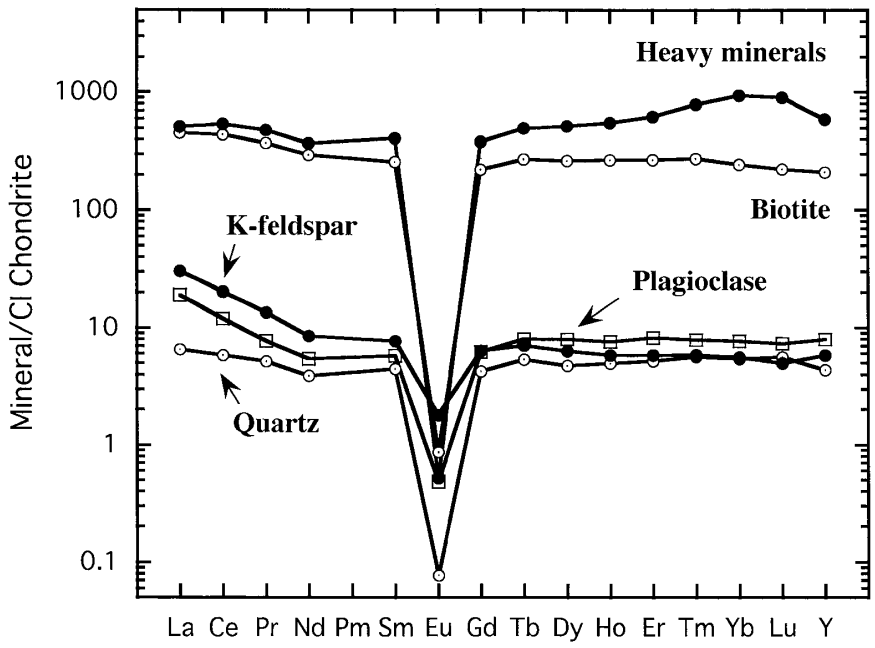

Fig. 7 The chondrite-normalized REE patterns for mineral separates of a Naegi granite sample (NG9-1). Every mineral separate shows a convex (M-type) tetrad effect and a negative Eu anomaly more or less.

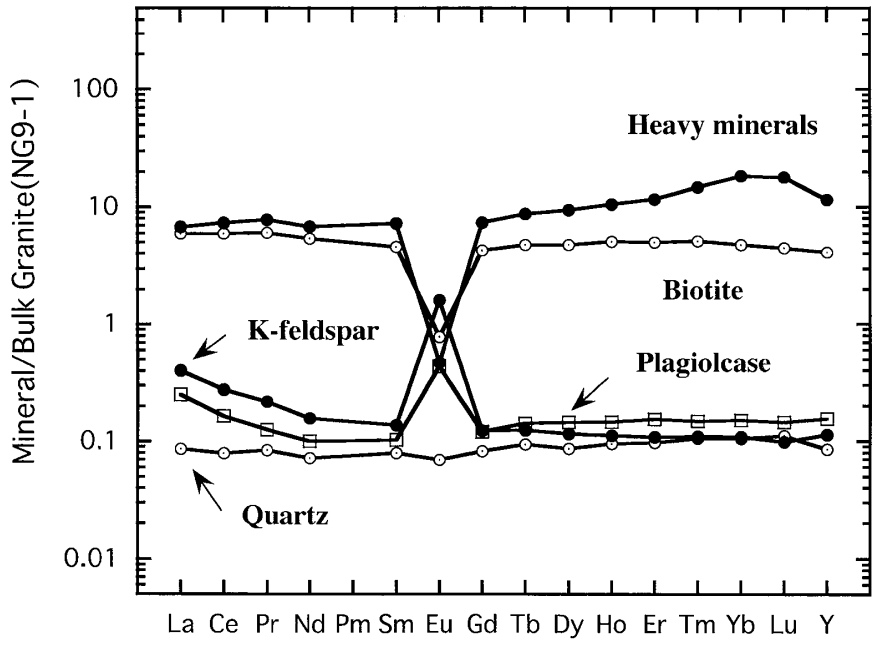

Fig. 8 The REE patterns for mineral separates normalized by the bulk granite (NG9-1) from which they have been separated. The vertical scale is the same as that in Fig. 7. Tetrad and octad effect variations become less apparent when compared with their chondrite-normalized patterns (Fig. 7), but the heavy minerals and biotite still exhibit subtle convex tetrad and octad effects. Plagiocalse and K-feldspar indicate positive Eu anomalies and light REE enrichment trends, which are frequently observed in granitic rocks.

5) REE fractionation among pegmatite, FMA and granite host

Here is examined the REE fractionation among pegmatite, FMA and host granite. The mutual REE enrichments in the three parts of pegmatite, FMS and host granite (NG10-1, FMA10-2, PG10-3) of the same specimen are shown in Fig. 9. The REE enrichment pattern of pegmatite relative to the host granite indicates a convex tetrad (M type) effect with a negative Eu anomaly and a heavy REE enrichment trend. In contrast, a concave (W type) tetrad effect is seen in the REE enrichment pattern of FMA relative to the host granite. This concave tetrad effect is related to the point we noted in Fig. 4. When FMA is normalized by the pegmatite, a concave tetrad effect with a positive Eu anomaly emerges. A similar relationship of REE enrichment is found in the other set of NG11-1, FMA11-2, PG11-3, though it is less obvious than the set shown in Fig. 9 and not shown here graphically.

The REE enrichment patterns for all the pairs of host granite/pegmatite in this study are shown in Fig. 10, where we can see concave (W type) tetrad effects with positive Eu anomalies and light REE enrichment trends. If the denominator of pegmatite is exchanged with the numerator of granite in Fig. 10, the pegmatite/granite pairs will show convex (M type) tetrad effects with negative Eu anomalies and heavy REE enrichment trends. Apart from the question which is a suitable normalizing material, pegmatite or granite, we would like to emphasize that most of the REE enrichment patterns for the pairs among pegmatite, FMA, and host granite exhibit much more obvious tetrad effects than their individual REE patterns normalized by chondrite. The REE distribution among the three texturally different parts may be an important constraint to our understanding how the tetrad effects were originated in the formation process of pegmatite-bearing granite suite.

According to Jahns and Burnham (1969), relatively fine-grained materials (FMA) are frequently found in the border zones between pegmatite and granite in many cases of granitic pegmatites, and it is conceivable that crystallization within the aqueous fluid-silicate melt system concomitantly yields relatively coarse-grained products from the aqueous phase and much fine-grained products from the coexistent melt, because material transfer rates in aqueous fluids are much more rapid than those in relatively viscous melt. If the coarse-grained pegmatite and FMA parts represent the crystallization products from aqueous fluid and silicate melt, respectively, the high-temperature aqueous fluid might have dissolved enough amounts of silicate components to crystallize the pegmatite which is almost the same silicate as the granite in mineralogy and bulk chemical composition. Even if the interpretation by Jahns and Burnham (1969) is accepted, this never signifies that the pegmatite and FMA parts preserve the respective chemical compositions of aqueous fluid and silicate melt. The pronounced negative Eu anomalies of all the chondrite-normalized REE patterns for granite, FMA and pegmatite parts (Figs. 2, 3, and 3) are the evidence for significant fluid escape from the Naegi granitic magma system. The heavy REE enrichment trends of pegmatite and FMA relative to the host granite may also be resulted from the escape of fluid with a positive Eu anomaly and light REE enrichment relative to the chondritic abundances. Much larger negative Eu anomalies of pegmatite samples than those of the host granite ones mean that the effect of fluid escape is more significantly reflected in the pegmatite rather than in the host granite.

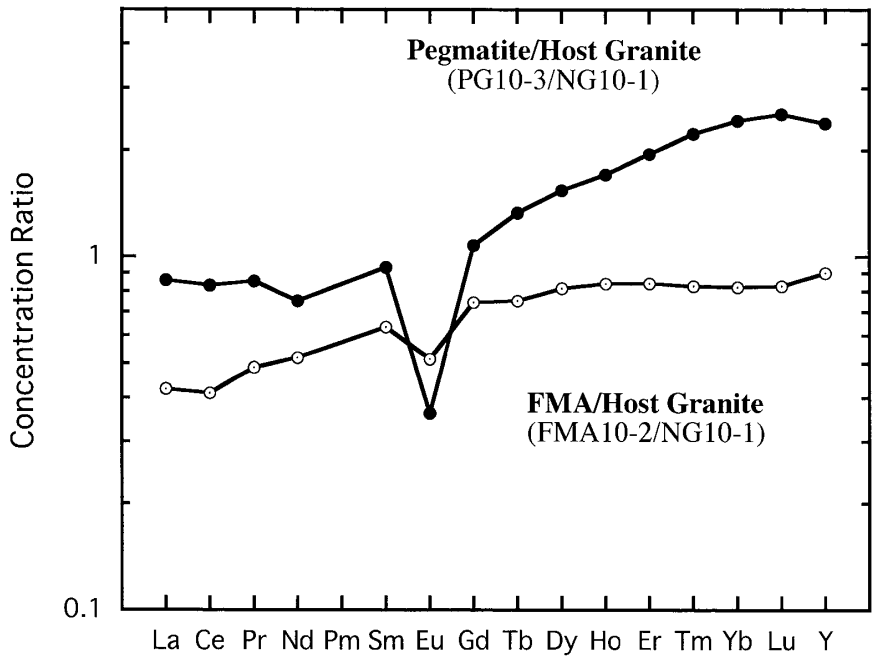

Fig. 9 REE fractionation among pegmatite, FMA and host granite parts. REE enrichment patterns for the pegmatite and the fine-grained material (FMA) relative to the host granite suggest a convex (M-type) and concave (W-type) tetrad effect features, respectively.

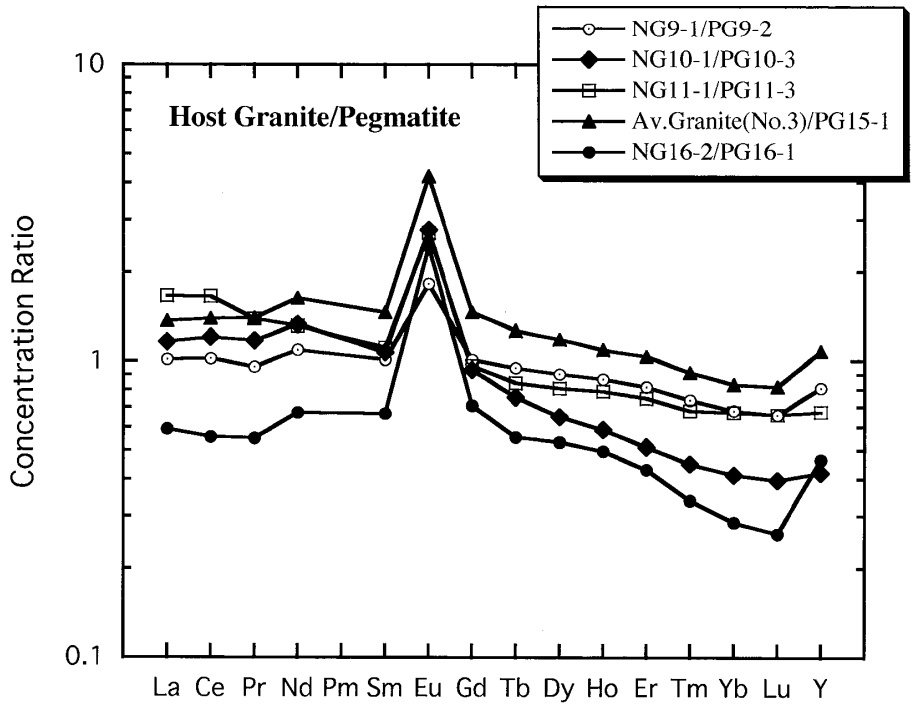

Fig. 10 REE enrichment patterns for host granites relative to respective pegmatites. The host granite for PG15-1 was not sampled, so that the averaged granite No. 3 is assumed to be the host granite part of PG15-1. There can be recognized concave (W-type) tetrad effects with positive Eu anomalies, together with light REE enrichment trends.

On the other hand, the field occurrence of pegmatite implies that pegmatite parts represent the residual silicates of relatively fluid-rich portions of hydrous felsic magma. Although it is not immediately certain whether such fluid was present as a discrete phase coexistent with melt or the dissolved fluid in melt, it is at least quite certain that the fluid has been lost from the magmatic system eventually. Two FMA samples (FMA10-2 and 11-2) are significantly depleted in REE relative to the respective host granite samples (Fig. 9). Hence, it might be a possible interpretation that FMA crystallized from the silicate melt in an immediate contact with the segregated fluid phase or from the fluid-depleted melt adjacent to the relatively fluid-rich melt.

Apart from specific interpretations of FMA, the texturally different parts of the pegmatite-bearing granite must be the traces of heterogeneous distribution of aqueous fluid within the hydrous granitic magma before substantial crystallization. This may also relate to the fluid segregation process in hydrous melt eventually. In addition, the fluid migration and fluid escape from the system must have been crucial to produce the huge negative Eu anomaly of every residual silicate. The pegmatite which we believe to be the residual silicate of fluid-rich melt, shows much larger negative Eu anomaly than the host granite. This point is very important when we interpret the fact that each host granite normalized by coexistent pegmatite indicates the REE enrichment pattern with a concave tetrad effect, a positive Eu anomaly and a light REE enrichment trend (Fig. 10). Our understanding of the results of Fig. 10 is as follows: Eventually the host granite inherits relatively more the fluid-like REE character from the original hydrous magma system than the pegmatite, because the fluid escape effect was more serious in the fluid-rich melt than the relatively fluid-poor melt to have crystallized the host granite. Additional discussion about this point will be made in the next subsection.

6) Origin of convex tetrad effects in evolved felsic rocks

The important role of water in granite genesis has been discussed repeatedly by many authors. For example, Whitney (1988) summarized how crystallization conditions are different between water-saturated and unsaturated granitic melt systems. However, the crystallization process does not appear immediately important in the discussion of the origin of tetrad effect, because the REE data for whole-rock samples and mineral separates of Naegi granite (Figs. 2 and 7) and Chinese Quanlishan and Baerzhe granites (Zhao *et al.*, 2002) indicate that convex tetrad effect existed in hydrous felsic magma before crystallization. Zhao *et al.* (2002) wrote for this situation that the fluid/melt interaction is the most important agent to produce the convex tetrad effect. Although their statement is acceptable, we would like to give a more specific statement that the convex tetrad effects in evolved felsic rocks originates in the combined process of segregation of aqueous fluid from hydrous felsic melt and its escape from the melt system.

Bureau and Keppler (1999) have demonstrated the complete miscibility of silicate melts with water in the *in-situ* observation experiments by diamond-anvil cell. This is important in considering the fluid segregation process in hydrous felsic melts. Although their experiments were carried out in the upper mantle conditions of the temperature and pressure ranges of 560–1000°C and 8–21 kbar, silicate melt is completely miscible

with water in a wide range of melt compositions including nepheline, jadeite, dacite, haplogranite and Ca-bearing granite. Bureau and Keppler (1999) also noted that even in a tholeiitic basalt/water system some evidence for complete miscibility has been obtained. The critical temperature of haplogranite is 1,003°C at 13.4 kbar, but under a higher pressure of 20.4 kbar the critical temperature decreases to 735°C. Unmixing of fluid and silicate melt occurs below the critical temperature at the given pressure, therefore the idea of fluid-saturated silicate melts is valid only in subcritical conditions, but it is not valid in the supercritical conditions at all. Even if homogeneous hydrous felsic magma is formed in the supercritical condition, the magma undergoes unmixing of fluid-rich and fluid-poor phases as it ascends into earth's crust. Hence segregation of fluid from hydrous felsic melt is inevitable, and then the partitioning of REE between the two phases becomes important as exemplified by the experimental K_d(REE: fluid/melt) in Flynn and Burnham (1978).

The K_d(REE: fluid/melt) values for the closed melt system, however, cannot explain the huge negative Eu anomalies at all, and this is also unable to explain the tetrad effect characteristics of REE abundance patterns for whole-rock samples and the relative REE enrichment patterns between pegmatite and host granite pairs. As discussed in Kawabe (1995) it is difficult to expect large tetrad effects in log[K_d(REE: fluid/melt)] at the high temperatures of magmatic conditions. There must be a certain mechanism to magnify small tetrad effects of log[K_d(REE: fluid/melt)] in residual silicates. Such a magnification mechanism is the fluid loss process as outlined in Kawabe (1995). One of the simplest model for it is the fractional loss of fluid from hydrous felsic melt, namely, the Rayleigh fractionation. The REE concentration in the residual silicate melt in the process can be given by the following equation as far as constant K_d(REE: fluid/melt) are assumed;

$$\log[(\mathrm{REE})/(\mathrm{REE})_0] = [K_d(\mathrm{REE}: \text{ fluid/melt}) - 1] \cdot \log(f_m), \quad (1)$$

where (REE) and $(\mathrm{REE})_0$ denote the REE concentrations in the residual silicate melt and the initial hydrous melt, respectively. The term of f_m (≤ 1) stands for the residual mass fraction of hydrous melt. When REE concentrations in hydrous melts to have produced pegmatite and host granite parts are compared after applying eq. (1) to them, we have the following equation:

$$\log[(\mathrm{REE})_G/(\mathrm{REE})_P] = [K_d(\mathrm{REE}: \text{ fluid/melt}) - 1] \cdot \{\log(f_m)_G - \log(f_m)_P\} + \log[(\mathrm{REE})_{0,G}/(\mathrm{REE})_{0,P}], \quad (2)$$

where the suffixes of G and P denote the melts to crystallize granite and pegmatite, respectively. This can be rewritten as the equation to give K_d(REE: fluid/melt) in terms of $\log[(\mathrm{REE})_G/(\mathrm{REE})_P]$,

$$K_d(\mathrm{REE}: \text{ fluid/melt}) = 1 + \log[(\mathrm{REE})_G/(\mathrm{REE})_P]/\log[(f_m)_G/(f_m)_P] - \log[(\mathrm{REE})_{0,G}/(\mathrm{REE})_{0,P}]/\log[(f_m)_G/(f_m)_P]. \quad (3)$$

If $(\mathrm{REE})_{0,G} \approx (\mathrm{REE})_{0,P}$, namely, the REE concentrations in the two initial melts are not so different,

$$K_d(\mathrm{REE}: \text{ fluid/melt}) \approx 1 + \log[(\mathrm{REE})_G/(\mathrm{REE})_P]/\log[(f_m)_G/(f_m)_P]. \quad (4)$$

Equation (4) may explain the reason why we normalized host granite by pegmatite in Fig. 10.

By assuming an appropriate value of $[(f_m)_G/(f_m)_P]$ in (4), a set of K_d(REE: fluid/melt) can be evaluated from the values of $\log[(REE)_G/(REE)_P]$ shown in Fig. 10. We interpret that the amount of fluid lost from the pegmatite part is greater than that from the adjacent granite part, so that it follows that $1< [(f_m)_G/(f_m)_P] < \infty$. When $[(f_m)_G/(f_m)_P]$ increases to infinity, all the K_d(REE: fluid/melt) values approach unity. When $[(f_m)_G/(f_m)_P]$ is close to unity, the right-hand side of (4) gives negative values for the cases that $[(REE)_G/(REE)_P] < 1$. This cannot be accepted, because K_d(REE: fluid/melt) $\geqq 0$ by the definition of partition coefficients. Therefore we input the values increasing from unity into $[(f_m)_G/(f_m)_P]$ of (4), and checked how the sets of K_d(REE: fluid/melt) values are resulted from the respective $[(REE)_G/(REE)_P]$ shown in Fig. 10. Although the five sets of $[(REE)_G/(REE)_P]$ cannot give a unique set of converged values of K_d(REE: fluid/melt), they gives a fairly narrow range of K_d(REE: fluid/melt) values by assuming specific values of $[(f_m)_G/(f_m)_P]$ for the respective sets of $[(REE)_G/(REE)_P]$. The estimated sets of K_d(REE: fluid/melt) are shown in Fig. 11-A, in which assumed $[(f_m)_G/(f_m)_P]$ values for respective sets of $[(REE)_G/(REE)_P]$ are shown as f's in the respective legends. The five sets of empirical K_d(REE: fluid/melt) are fairly similar with each other. In particular, the three sets of $[(REE)_G/(REE)_P]$ shown by the filled symbols in Fig, 11-A give subparallel variation patterns across the series and showing similar small concave tetrad effects, small positive Eu anomalies, and light REE enrichment trends (Fig. 11-B).

In spite of our simple model assuming K_d(REE: fluid/melt) independent of (f_m) and $(REE)_{0,G} \approx (REE)_{0,P}$, the results of Figs. 11-A and B seem plausible in view of small regular concave tetrad effects in $\log K_d$(REE: fluid/melt). Figure 12 compares our empirical K_d(REE: fluid/melt) with the experimental ones reported by Flynn and Burnham (1978) and Ayers and Eggler (1995). Flynn and Burnham (1978) reported the experimental K_d (REE: fluid/melt) with REE=Ce, Eu, Gd and Yb at 4 kbar and 800°C, in which the chloride concentration in fluid was changed in the range of m(Cl) = 0.64 – 0.91(mol/kg). The experimental K_d (REE: fluid/melt) values show positive Eu anomalies and light REE enrichment trends similar to those in our empirical ones, but they are one order of magnitude smaller than our empirical values. Flynn and Burnham (1978), however, found that K_d (REE: fluid/melt) increases with increasing chloride concentration in the fluid phase. They argued that experimental K_d (REE: fluid/melt) except REE=Eu increases in the third power of chloride concentration. Webster *et al.* (1989) published experimental K_d (M: fluid/melt) with M=Ce, Y and other metals at 2 kbar and 800–950°C and solutions having variable m(Cl) up to 6 (mol/kg). The results supported partly the cubic law in the case of K_d(Ce: fluid/melt), where K_d (Ce: fluid/melt) values greater than unity have been obtained. On the other hand, Ayers and Eggler (1995) reported K_d (REE: fluid/melt) with REE=La, Sm, Tm and Y at 1,250°C with 15 and 20 kbar pressures using aqueous solutions of m(NaCl)=1.5 and 3 (mol/kg). The resultant K_d(REE: fluid/melt) values range from 0.4 to 0.7, which are closer to our empirical estimates (Fig. 12), although it is impossible to inspect the tetrad effect in the experimental K_d(REE: fluid/melt) for the limited number of REE. The experimental K_d(REE: fluid/melt) values are suggesting that K_d(REE: fluid/melt) is

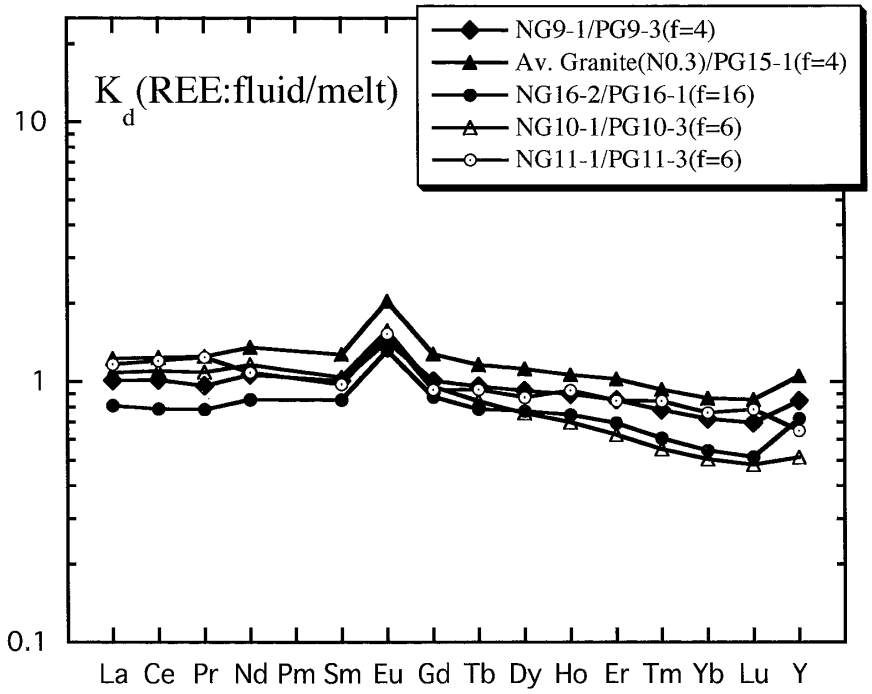

Fig. 11-A K_d(REE: fluid/melt) sets evaluated from the granite/pegmatite pairs shown in Fig. 10 and eq. (4). The f values shown in the respective legends correspond to the assumed parameter values of $(f_m)_G/(f_m)_P$ in eq. (4).

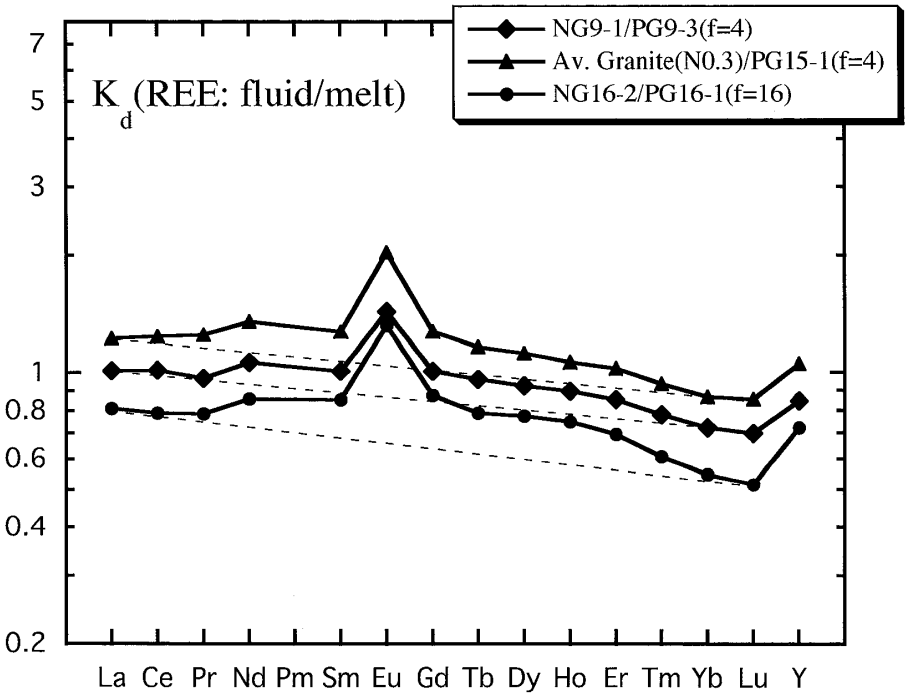

Fig. 11-B Estimated sets of K_d(REE: fluid/melt) from three pairs of granite/pegmatite based on eq. (4). The f values in the respective legends correspond to the assumed $(f_m)_G/(f_m)_P$ values in eq. (4). The series variations of $\log K_d$(REE: fluid/melt) show concave (W type) tetrad effects with small positive Eu anomalies, together with gentle trends of light REE enricment. Note that tetrad effects of $\log K_d$(REE: fluid/melt) are more regular and symmetric than those of log(granite/pegmatite) shown in Fig. 10.

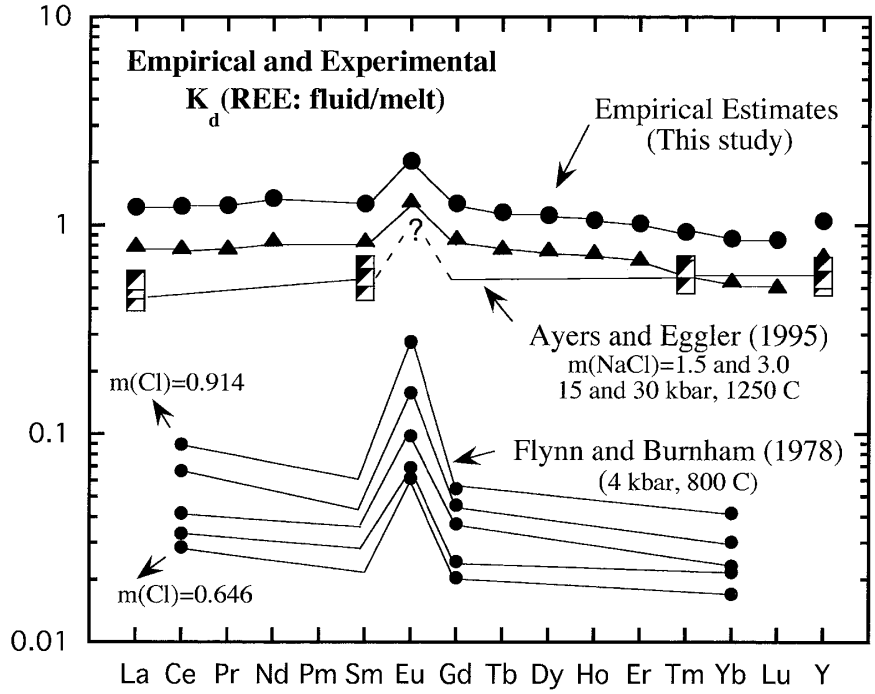

Fig. 12 The empirical estimates of K_d(REE: fluid/melt) in this study compared with experimental K_d(REE: fluid/melt) values reported by Flynn and Burnham (1978) and Ayers and Eggler (1995). The empirical estimates are by the pairs of NG16-2/PG16-1 (f=16) and the average granite No. 3/PG15-1 (f=4) in Fig. 11-B.

affected by chemical composition of fluid, in particular, K_d(REE: fluid/melt) increases with increasing chloride concentration. Although it is impossible to make rigorous evaluation of our empirical K_d(REE: fluid/melt) values by using the experimental K_d(REE: fluid/melt) values at the present stage, our empirical estimates of K_d(REE: fluid/melt) do not contradict the experimental results by Ayers and Eggler (1995) or even those by Flynn and Burnham (1978) when the nature of K_d(REE: fluid/melt) depending on chloride concentration is taken into consideration.

The REE study of Naegi granite-pegmatite suite has provided a simple model for the convex tetrad effect associated with huge negative Eu anomaly in evolved felsic rocks: Fractional loss of fluid from a hydrous felsic melt system leaves residual silicate melts in which the small concave tetrad effect and a positive Eu anomaly of log K_d(REE: fluid/melt) can be exaggerated in the reversed manners, namely, the residual silicate melts acquire the REE abundance characteristics of pronounced convex tetrad effects and huge negative Eu anomalies. Such melts eventually solidify as differentiated felsic rocks we encounter in the field.

CONCLUSIONS

The following conclusions have been drawn from the REE study of Naegi granite-pegmatite suite:

(1) The pegmatite sparsely occurs as small patches with sizes less than 20 cm in the Naegi granite body. The ganite and pegmatite samples indicate convex tetrad effects

and huge negative Eu anomalies of Eu/Eu* = 0.02–0.004 in their chondrite-normalized REE patterns. Mineral separates (quartz, plagioclase, K-feldspar, biotite, and residual heavy minerals) from a granite sample, also show similar REE characteristics to those of the whole-rock granite sample. Accordingly the original magma before crystallization had been characterized by the REE abundances with convex tetrad effect.

(2) The granite and pegmatite samples show no significant differences in major element chemistry and mineralogy except the mineral size and texture, but the pegmatite is depleted in Sr, Ba and Eu relative to the granite. The field occurrence of pegmatite suggests a heterogeneous distribution of aqueous fluid inside of the granitic magma. Possibly this may be related to the unmixing phenomenon of fluid and silicate melt. Significant REE fractionation is recognized between the pairs of pegmatite and host granite. Concave tetrad effects, positive Eu anomalies, and ligh REE enrichment trends emerge when host granite samples are normalized by respective pegmatite ones.

(3) A simple model of fractional loss of fluid from a hydrous felsic melt has been proposed in order to explain the REE data for the Naegi granite and pegmatite suite. By applying the model to the observed REE fractionation between pegmatite and granite pairs, the REE partition coefficients between aqueous fluid and melt phases, K_d(REE: fluid/melt), have been evaluated. The sets of K_d(REE: fluid/melt) values display small regular convex tetrad effects, positive Eu anomalies, and light REE enrichment trends.

(4) Fractional loss of fluid from a hydrous felsic melt system leaves behind residual silicate melts, in which the small concave tetrad effect and positive Eu anomaly of log K_d(REE: fluid/melt) can be magnified in the reversed manners, namely, the REE abundance characteristics of pronounced convex tetrad effects and huge negative Eu anomalies are acquired by the residual silicates.

ACKNOWLEDGEMENTS

The authors thank T. Obayashi, Nakatsugawa Mineral Museum, for his kind guidance as to the occurrence of Naegi granite, K. Suzuki and K. Yamamoto, Nagoya Univ., for their permission to use XRF facility, and T. Okuchi, Nagoya Univ., for his instruction as to the experimental works of miscibility of water with silicate melts. Thanks are due to T. Tanaka and other members of Geochemistry Laboratory, Nagoya Univ., for their advice and supports on REE analysis and mineral separation. This works was supported partly by the grants Nos. 03402018 and 06453007 from the Ministry of Education, Science and Culture, Japan to I.K., and also partly by the grant-in-aid (No. 14901241) from Japan Society for Promotion of Science to I.K.

REFERENCES

Anders, E. and Grevesse, N. (1989) Abundances of the elements: Meteoritic and solar. *Geochim. Cosmochim. Acta*, **53**, 197–214.

Ayers, J.C. and Eggler, D.H. (1995) Partitioning of elements between silicate melt and H_2O-NaCl fluids at 1.5 and 2.0 GPa pressure: Implications for mantle metasomatism. *Geochim. Cosmochim. Acta*, **59**, 4237–4246.

Bau, M. (1996) Controls on the fractionation of isovalent trace elements in magmatic and aqueous

systems: evidence from Y/Ho, Zr/Hf, and lanthanide tetrad effect. *Contrib. Mineral. Petrol.* **123**, 323–333.

Bureau, H. and Keppler, H. (1999) Complete miscibility between silicate melts and hydrous fluids in the upper mantle: experimental evidence and geochemical implications. *Earth Planet. Sci. Lett.* 165, 187–196.

Caro, P., Deroouet, J., Beaury, L., Teste de Sagey, G., Chaminade, J.P., Aride, J. and Pouchard, M.J. (1981) Interpretation of the optical absorption spectrum and paramagnetic susceptibility of neodymium trifluoride. *J. Chem. Phys.* **74**, 2698–2704.

Drake, M.J. and Weill, D.J. (1975) Partition of Sr, Ba, Ca, Y, Eu^{2+}, Eu^{3+} and other REE between plagioclase feldspar and magmatic liquid: an experimental study. *Geochim. Cosmochim. Acta*, **39**, 689–712.

Flynn, R.T. and C.W. Burnham (1978) An experimental determination of rare earth partition coefficients between a chloride containing vapor phase and silicate melts. *Geochim. Cosmochim. Acta*, **42**, 658–701.

Henderson, P. (1984) General geochmeical properties and abundances of the rare earth elements. In: (Editor, Henderson, P.) *Rare Earth Element Geochemistry*, 1–32, Elsevier.

Irber, W. (1999) The lanthanide tetrad effect and its correlation with K/Rb, Eu/Eu*, Sr/Eu, Y/Ho, and Zr/Hf of evolving peraluminous granite suites. *Geochim. Cosmochim. Acta*, **63**, 489–508.

Jahn, B.M., Wu, F., Capdevila, R., Martineau, F., Zhao, Z. and Wang, Y. (2001) Highly evolved juvenile granites with tetrad REE patterns: the Woduhe and Baerzhe granites from Great Xing'an Mountains in NE China. *Lithos*, **39**, 171–198.

Jahns, R.H. and Burnham, W. (1969) Experimental studies of pegmatite genesis: I. A model for the derivation and crystallization of granitic pegmatites. *Econ. Geol.*, **64**, 843–864.

Jørgensen, C.K. (1979) Theoretical chemistry of rare earths. In: *Handbook on the Physics and Chemistry of Rare Earths* (Editors, Gschneider, K.A. Jr. and Eyring, L.), **3**, 111–169, North-Holland, Amsterdam.

Jørgensen, C.K. (1970) The "Tetrad effect" of Peppard is a variation of the nephelauxetic ratio in the third decimal. *J. inorg. nucl. Chem.*, **32**, 3127–3128.

Jørgensen, C.K. (1962) Electron transfer spectra of lanthanide complexes, *Mol. Phys.* **5**, 271–277.

Kawabe, I. (1995) Tetrad effect and fine structures of REE abundance patterns of granitic and rhyolitic rocks: ICP-AES determinations of REE and Y in eight GSJ reference rocks. *Geochem. J.* **29**, 213–230.

Kawabe, I. (1992) Lanthanide tetrad effect in the Ln^{3+} ionic radii and refined spin-pairing energy theory. *Geochem. J.* **26**, 309–335.

Kawabe, I. and Masuda, A. (2001) The original examples of lanthanide tetrad effect in solvent extraction: A new interpretation compatible with recent progress in REE geochemistry. *Geochem. J.*, **35**, 215–224.

Kawabe, I., Toriumi, T., Ohta, A., and Kanda, S. (1995) Effective application of ultrasonic nebulizer to ICP-AES analysis of REE, Y and Sc in geochemical samples. *J. Earth Planet. Sci. Nagoya Univ.*, **42**, 1–15.

Lee, S.M., A. Masuda, and H.S. Kim (1994) An early Proterozoic leuco-granitic gneiss with the REE tetrad phenomenon. *Chem. Geol.* **114**, 59–67.

Masuda, A. and Akagi, T. (1989) Lanthanide tetrad effect observed in leucogranites from China. *Geochem. J.* **23**, 245–253.

Masuda, A., O. Kawakami, Y. Dohmoto, and T. Takenaka (1987) Lanthanide tetrad effect in nature: two mutually opposite types, W and M. *Geochem. J.* **21**, 119–124.

McKay, G.A. (1989) Partitioning of rare earth elements between major silicate minerals and basaltic melts. *Rev. Mineral.* **21**, 45–77.

Michard, A. (1989) Rare earth element systematics in hydrothermal fluids. *Geochim. Cosmochim. Acta*, **53**, 745–750.

Monecke, T., Kempe, U., Monecke, J., Sala, M. and Wolf, D. (2002) Tetrad effect in rare earth element distribution patterns: A method of quantification with application to rocks and mineral samples from granite-related rare metal deposits. *Geochim. Cosmochim. Acta*,

66, 1185–1196.

Nugent, L.J. (1970) Theory of the tetrad effect in the lanthanide(III) and actinide(III) series. *J. inorg. nucl. Chem.*, **32**, 3485–3491.

Peppard, D.F., Mason, G.W., and Lewey, S. (1969) A tetrad effect in the liquid-liquid extraction ordering of lanthanides (III). *J. inorg. nucl. Chem.* **31**, 22712272.

Reisfeld, R. and Jørgensen, C.K. (1977) *Lasers and Excited States of Rare Earths*, Springer, Berlin, 226 pp.

Shibata, K., Miller, J.A., Yamagda, N., Kawata, K., Murayama, M. and Katada, M. (1962) Pottasium-Argon ages of the Inagawa Granite and Naegi Granite. *Bull. Geol. Surv. Japan*, **13**, 317–320.

Suzuki, K., Morishita, T., Kajizuka, I., Nakai, Y., Adachi, M. and Shibata, K. (1994) CHIME ages of monazites from the Ryoke metamorphic rocks and some granitoids in the Mikawa-Tono area, central Japan. *Bull. Nagoya Univ. Furukawa Museum*, **10**, 17–38.

Sverjensky, D.A. (1984) Europium redox equilibria in aqueous solution. *Earth Planet. Sci. Lett.*, **67**, 70–78.

Takahashi, Y., Yoshida, H., Sato, N., Hama, K., Yusa, Y. and Shimizu, H. (2002) W-and M-type tetrad effects in REE patterns for water-rock systems in the Tono uranium deposit, central Japan. *Chem. Geol.* **184,** 311–335.

Takahashi, T. and Kawabe, I. (2003) Lanthanide tetrad effects in Naegi granite and pegmatite, central Japan. *Geochim. Cosmochim. Acta*, **67**, no. 18 (S1), *Abst. 13th Ann. V. M. Goldschmidt Conf.* , A469L.

Tanimizu, M. and Tanaka, T. (2002) Coupled Ce-Nd isotope systematics and rare earth elements differentiation from the moon. *Geochim. Cosmochim. Acta*, **66**, 4007–4012.

Webster, J.D., Holloway, J.R. and Hervig, R.L. (1989) Partitioning of lithophile trace elements between H_2O and H_2O+CO_2 fluids and topaz rhyolite melt. *Econ. Geol.* **84**, 116–134.

Whitney, J.A. (1988) The origin of granite: The role and source of water in the evolution of granitic magmas. *Geol. Soc. Am. Bull.*, **100**, 1886–1897.

Yamamoto, K., Yamashita, F. and Adachi, M. (2005) Precise determination of REE for sedimentary reference rocks issued by the Geological Survey of Japan. *Geochem. J.*, **39**, 289–297.

Zhao, Z., Masuda, A. and Shabani, M.B. (1992) REE tetrad effects in rare metal granite. *Chinese J. Geochem.* **12**, 221–233.

Zhao, Z., Xiong, X., Han, X., Wong, Y., Wong, Q., Bao, Z. and Jahn, B.M. (2002) Controls on the REE tetrad effect in granites: Evidence from the Qianllishan and Baerzhe granites, China. *Geochem. J.*, **36**, 527–543.